Am J Cancer Res 2022;12(7):3280-3293
www.ajcr.us /ISSN:2156-6976/ajcr0143092

Original Article

Bortezomib- and carfilzomib-resistant myeloma cells show increased activity of all three arms of the unfolded protein response

Tadeusz Kubicki[1], Kinga Bednarek[2], Magdalena Kostrzewska-Poczekaj[2], Magdalena Luczak[3], Krzysztof Lewandowski[1], Lidia Gil[1], Malgorzata Jarmuz-Szymczak[1,2], Dominik Dytfeld[1]

[1]Department of Hematology and Bone Marrow Transplantation, Poznan University of Medical Sciences, Poznan, Poland; [2]Institute of Human Genetics, Polish Academy of Sciences, Poznan, Poland; [3]Institute of Bioorganic Chemistry, Polish Academy of Sciences, Poznan, Poland

Received March 24, 2022; Accepted June 25, 2022; Epub July 15, 2022; Published July 30, 2022

Abstract: Proteasome inhibitors are among the most potent classes of drugs in multiple myeloma treatment. One of the main challenges in myeloma therapy is acquired resistance to drugs. Several theories have been proposed to describe the mechanisms responsible for resistance to the most commonly used proteasome inhibitors bortezomib and carfilzomib. This study aimed to describe functional differences between sensitive myeloma cells (MM1S WT) and their daughter cell lines resistant to either bortezomib (MM1S/R BTZ) or carfilzomib (MM1S/R CFZ), as well as between both resistant cell lines. Bortezomib- and carfilzomib-resistant cell lines were successfully generated by continuous exposure to the drugs. When exposed to different drugs than during the resistance generation period, MM1S/R BTZ cells showed cross-resistance to carfilzomib, whereas MM1S/R CFZ cells were similarly sensitive to bortezomib as MM1S WT cells. Following proteomic profiling, unsupervised principal component analysis revealed that the MM1S/R BTZ and MM1S/R CFZ cell lines differed significantly from the MM1S WT cell line and from each other. Canonical pathway analysis showed similar pathways enriched in both comparisons - MM1S WT vs. MM1S/R CFZ and MM1S WT vs. MM1S/R BTZ. However, important differences were present in the statistical significance of particular pathways. Key alterations included the ubiquitin-proteasome system, metabolic pathways responsible for redox homeostasis and the unfolded protein response. In functional studies, both drugs continued to reduce chymotrypsin-like proteasome activity in resistant cells. However, the baseline activity of all three catalytic domains of the proteasome was higher in the resistant cells. Differences in generation of reactive oxygen species were identified in MM1S/R BTZ (decreased) and MM1S/CFZ cells (increased) in comparison to MM1S WT cells. Both baseline and drug-induced activity of the unfolded protein response were higher in resistant cells than in MM1S WT cells and included all three arms of this pathway: IRE1α/XBP1s, ATF6 and EIF2α/ATF4 (downstream effectors of PERK). In conclusion, contrary to some previous reports, resistant MM1S cells show upregulation of unfolded protein response activity, reflecting the heterogeneity of multiple myeloma and prompting further studies on the role of this pathway in resistance to proteasome inhibitors.

Keywords: Multiple myeloma, resistance, bortezomib, carfilzomib, unfolded protein response, proteasome, proteomics

Introduction

Multiple myeloma (MM) is a blood cancer caused by malignant transformation of plasma cells. In recent years, tremendous progress has been achieved in the treatment of this disease; however, MM still remains incurable [1]. While the vast majority of patients respond well to first-line treatment, relapses are inevitable, and with each subsequent regimen of therapy, remissions are more difficult to achieve and last for less time [2], attributed to complex alterations in cell biology leading to acquired resistance to treatment.

Proteasome inhibitors (PIs) are among the most potent and commonly used antimyeloma agents. Currently, there are three approved drugs in this class - bortezomib, carfilzomib and ixazomib [3-5]. These drugs all take advantage

of the extremely high protein synthesis rate present in MM cells. By blocking different proteasome subunits (bortezomib reversibly blocks β5, carfilzomib irreversibly blocks β5, β2 and β1, and ixazomib reversibly blocks β5 and β1) the drugs expose MM cells to fatal proteotoxic stress [6]. Despite being so potent in targeting the Achilles heel of MM, PIs are also susceptible to acquired resistance that develops over time. Several potential mechanisms responsible for this phenomenon have been proposed in recent years, including mutations in the protein encoding proteasome subunit β5c (PSMB5) [7], alterations in cell metabolism [8] and changes in unfolded protein response (UPR) pathway activity [9].

Recently, mutations in PSMB5 that lead to a decreased ability of PIs to block the proteasome have been confirmed in a very small percentage of MM patients and therefore are not considered a key pathogenetic driver of resistance to this class of drugs [10]. A more promising explanation includes complex changes in MM cell metabolism leading to an increase in antioxidant capacity, accomplished by enhanced glycolysis, decreased activity of pathways responsible for lipid biosynthesis and overproduction of antioxidant proteins [8, 9, 11, 12]. Redox homeostasis is critical for appropriate protein folding in the endoplasmic reticulum (ER) and thus can significantly affect UPR pathway activity [13].

The UPR is an adaptive pathway triggered in response to increased ER stress caused by the overaccumulation of misfolded proteins [14]. There are three arms of this pathway, represented by three proteins acting as signal transducers (PERK, IRE1, ATF6). These molecules reside in the ER membrane and, under physiological conditions, are kept inactive due to binding BiP/Grp78 protein to their intraluminal sites. When misfolded proteins accumulate in the ER lumen, BiP dissociates from the transducers, leading to their activation and initiation of the UPR. Three pathways act simultaneously to counteract ER stress by attenuating global protein synthesis, enhancing cell folding capacity and increasing the ability to destroy misfolded proteins. The UPR aims to restore homeostasis; however, when proteotoxicity overwhelms the adaptive abilities of cells, the pathway initiates apoptosis - this situation occurs in sensitive cells after exposure to PIs [15]. Several studies suggest that PI-resistant cells are characterized by decreased UPR activity, namely, one of the three main regulatory switches, the IRE1/XBP1 axis [9, 16, 17].

However, some assumptions proposed in the IRE1/XBP1-low model have recently failed to be reproduced, and there is still a knowledge gap regarding differences in resistance mechanisms to different types of PIs [18].

Herein, we present the results of a comprehensive proteomic and functional comparison of MM cells with acquired resistance to bortezomib or carfilzomib, the two most commonly used PIs. We describe several differences at the proteome level that result in functional alterations between the two cell lines and attempt to unravel the association of UPR activity with resistance to PIs.

Materials and methods

Cell culture

The MM1S human multiple myeloma cell line was purchased from American Tissue Culture Collection (CRL-2974™, ATCC, Manassas, VA, USA). Cells were cultured in Roswell Park Memorial Institute (RPMI)-1640 medium supplemented with 10% fetal bovine serum (FBS), 100 U/mL penicillin, and 100 mg/mL streptomycin. To generate resistance to bortezomib (S1013, Selleck Chemicals, Houston, TX, USA) or carfilzomib (S2853, Selleck Chemicals), MM1S cells were continuously coincubated with increasing concentrations of the drugs for 12-24 months. Resistance was defined as at least a 2-fold increase in the half maximal inhibitory concentration (IC_{50}) following a 24-hour incubation with the drugs, and the resistance factor was calculated by dividing the IC_{50} value of the resistant line by the IC_{50} of the sensitive line. After confirming the resistance status of the cells, all subsequent experiments were performed after a 14-day washout period in drug-free medium.

Cell viability assay

The changes in viability of both sensitive and PI-resistant cell lines in response to bortezomib and carfilzomib were measured using a commercially available colorimetric assay (Cell

Counting Kit-8, CCK-8, Sigma, St. Louis, MO, USA) according to the manufacturer's instructions. The absorbance of the culture medium with cells was measured at 450 nm and 600 nm using a GloMax microplate reader (GloMax Multi Detection System, Promega, Madison, WI, USA). Two independent experiments were performed in triplicate, and the results are presented as the mean ± standard deviation (SD). The IC_{50} value was calculated by curve fitting using quadratic regression.

Proteomics

Protein preparation and nano-liquid chromatography-tandem mass spectrometry (LC-MS/MS) analysis: The cell pellets (5×10^5 cells) were obtained from MM1S WT cells and cells that were able to grow in 6 nM bortezomib (MM1S/R BTZ) and in 8 nM carfilzomib (MM1S/R CFZ). The pellets were homogenized using a Precellys24 homogenizer (Bertin Instruments, Montigny-le-Bretonneux, France). Next, the samples were sonicated on ice for 10 min using an ultrasonic bath. The samples were centrifuged, and the supernatants were used for protein concentration assays (bicinchoninic acid (BCA) Protein Assay Kit, Thermo Fisher Scientific, Waltham, MA, USA). Ten micrograms of protein mixture was reduced with 5.6 mM DTT for 5 min at 95°C and then alkylated with 5 mM iodoacetamide for 20 min at room temperature (RT). The samples were digested with 0.2 µg of trypsin (Promega) overnight at 37°C. The samples were analyzed by nanoLC-MS/MS using a Dionex UltiMate 3000 RSLCnano System coupled with a Q-Exactive Orbitrap mass spectrometer (Thermo Fisher Scientific) in one batch as described [19]. Following LC-MS/MS analysis, the raw files were analyzed to evaluate the quality of the performed runs by Proteome Discoverer (PD), version 2.2.0.388 (Thermo Fisher Scientific). The reproducibility of the biological and technical replicates was assessed by scatter plotting, and the correlation coefficient was determined based on the label-free quantification (LFQ) intensities. Only samples with Pearson correlation coefficients above 0.8 were included in the quantitative surveys.

Quantitative analysis of proteomic data

The raw files were quantitatively analyzed by PD software with the Sequest engine. The identification of proteins at ≤ 1% false discovery rate (FDR) was performed against the UniProt complete human proteome set using the following parameters: a tolerance level of 10 ppm for MS and 0.08 Da for MS/MS, and two missed cleavages were allowed. The carbamidomethylation of cysteines was set as a fixed modification, and the oxidation of methionine was allowed as a variable modification. The analysis of the samples was based on the normalized PD intensities. Only proteins detected in all samples were considered in the quantitative analyses (no missing values). The fold changes in the level of the proteins were assessed by comparing the mean intensities among all experimental groups. Statistical analyses were performed using Perseus 1.6.1.3. The data were statistically analyzed using Student's unpaired *t*-test, and more than two groups were compared using one-way analysis of variance (ANOVA) with FDR correction. Statistical significance was accepted as $q < 0.05$. A protein was considered to be differentially expressed if the difference between at least 2 groups was statistically significant ($q < 0.05$) and the fold change was ≥ 2. Only differentially expressed proteins (DEPs) identified with a minimum of 2 unique peptides were accepted. Multivariate analyses were carried out by untargeted principal component analysis (PCA) and hierarchical clustering. For hierarchical clustering and heatmap visualization, data were normalized to the z-score.

Bioinformatic analysis

Bioinformatic analysis was conducted using Ingenuity Pathway Analysis software (Ingenuity Systems, Redwood City, CA, USA). All identified DEPs were annotated according to their Gene Ontology in the canonical pathway and biological function. Then DEPs (*q value* < 0.05; fold change ≥ 2; ≥ 2 unique peptides) were subjected to enrichment analysis to determine the top canonical pathways and biological functions associated with the observed differences in protein profiles. Enrichment analysis was performed using the right-tailed Fisher's exact test with Benjamini-Hochberg (B-H) multiple corrections. Based on the obtained *p value*, this test estimates the probability that the association between a set of molecules and a function or pathway is not random.

Table 1. Characteristics of antibodies used in Western blot experiments

Primary Abs				Secondary Abs		
Manufacturer	Cat. no	Antigene	Dilution	Manufacturer	Cat. no	Dilution
Cell signaling	9722	anti-eIF2a	1/1000	Cell signaling	7074	1/3000
Cell signaling	11815	anti-ATF-4	1/1000	Abcam	ab97051	1/35000
Cell signaling	83418	anti-XBP-1s	1/1000	Abcam	ab97051	1/5000
Abcam	ab122897	anti-ATF6	1/1000	Sigma	A9917	1/5000
Cell signaling	12721	anti-NRF2	1/1000	Abcam	ab97051	1/3000
Abcam	ab37073	anti-IRE1	0.4 ug/ml	Abcam	ab97051	1/50000
Abcam	ab48187	anti-phospho-IRE1	1/1500	Abcam	ab97051	1/50000
Abcam	ab9485	anti-GAPDH	1/10000	Abcam	ab97051	1/40000
Invitrogen	PA5-29444	anti-alpha Tubulin	1/5000	Abcam	ab97051	1/20000

Proteasome activity

Proteasome chymotrypsin-like, trypsin-like and caspase-like activities (reflecting the function of proteasome β5, β2 and β1 subunits, respectively) were measured using a commercially available kit - Cell-Based Proteasome-Glo™ 3-Substrate System (G1180, Promega) according to the manufacturer's instructions. The cell lines, both PI-sensitive and -resistant, were incubated for 4 and 6 hours in drug-free medium and different concentrations of bortezomib and carfilzomib (10, 20, 50 nM). The luminescence was measured using a GloMax microplate reader (GloMax Multi Detection System, Promega). Two independent experiments were performed in duplicate, and the results are presented as the mean ± SD.

Apoptosis

PI-resistant and -sensitive cell lines were cultured in different concentrations of bortezomib and carfilzomib (0, 5, 10, 50 nM). Next, apoptosis was assessed by measuring caspase-3 activity using a commercially available Caspase-3 Assay Kit (ab39401, Abcam, Cambridge, UK) according to the manufacturer's instructions. The absorbance was measured at 405 nm after 2 and 6 hours of incubation using a BioTek microplate reader (ELx808, BioTek, Winooski, VT, USA). Two independent experiments were performed in duplicate, and the results are presented as the mean ± standard deviation (SD).

Reactive oxygen species (ROS) generation

ROS generation in PI-resistant and -sensitive cells, baseline and in response to 6 hours of coincubation with different concentrations of bortezomib and carfilzomib (10, 20, 50 nM), was assessed by measuring the hydrogen peroxide concentration using a commercially available kit - ROS-Glo™ H_2O_2 Assay (G8820, Promega) according to the manufacturer's instructions. The luminescence was measured using a GloMax microplate reader (GloMax Multi Detection System, Promega). Two independent experiments were performed in duplicate, and the results are presented as the mean ± SD.

Western blot

After incubation of both sensitive and PI-resistant cells with different concentrations of PIs (0, 5, 10, 50 nM) for 2 and 6 hours, cells were lysed with radioimmunoprecipitation assay (RIPA) buffer (150 mM sodium chloride, 1% Triton X-100, 0.5% sodium deoxycholate, 0.1% sodium dodecyl sulfate (SDS), 50 mM tris (hydroxymethyl) aminomethane (TRIS) pH 8.0) with protease inhibitor cocktail (Lab Empire, Rzeszow, Poland). Protein concentration was assessed with the Bradford method [20]. Forty micrograms of total protein was denatured in 6× Laemmli buffer with 50 mM dithiothreitol (DTT) and loaded per lane of 4-15% polyacrylamide gel (Mini-PROTEAN TGX Stain-Free gels, Bio-Rad, Hercules, CA, USA). After SDS-polyacrylamide gel electrophoresis (PAGE), proteins were transferred to a 0.2 μm nitrocellulose membrane using a Trans-Blot Turbo Transfer System (BioRad, Mixed MW protocol). The membranes were blocked in 5% nonfat dry milk in tris-buffered saline with Tween (TBS-T) (0.1% Tween-20) for 1 h (RT). The primary and secondary antibody concentrations together with the time of incubation are listed in **Table 1**.

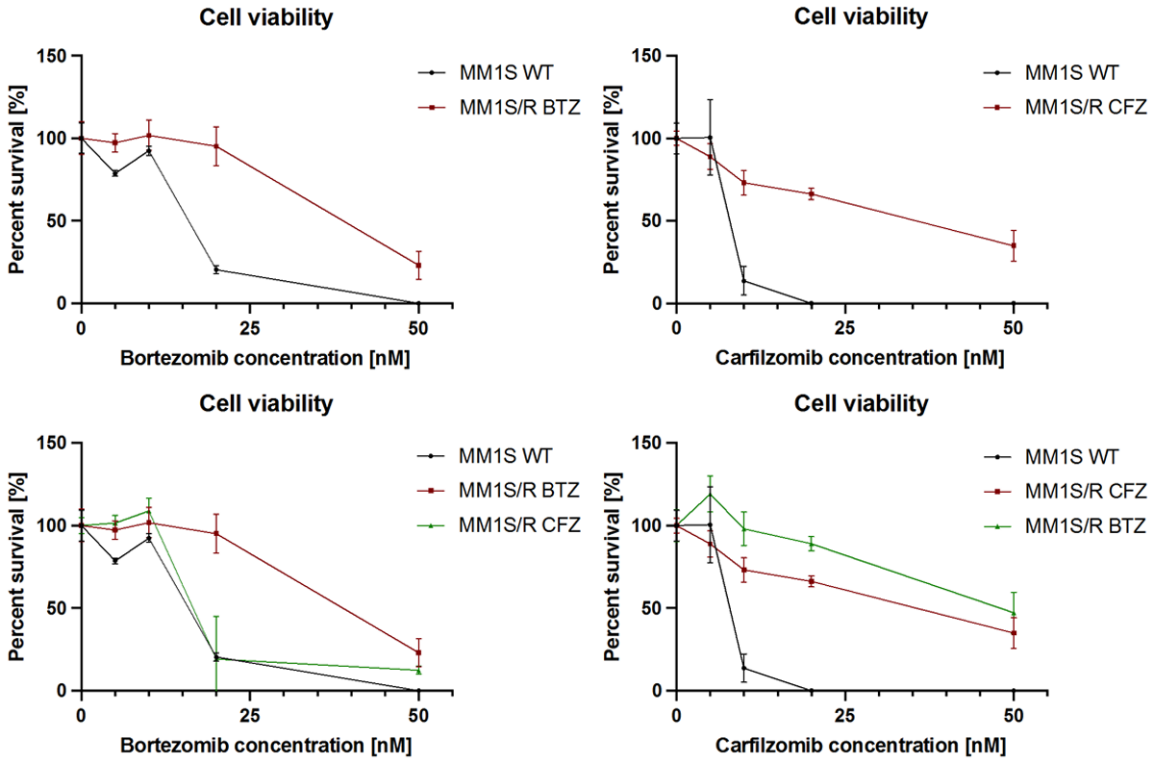

Figure 1. Effects of bortezomib and carfilzomib treatment on the viability of sensitive and resistant cells. Cells were continuously cultured for 24 hours with increasing concentrations of both drugs.

For protein detection, Clarity Western ECL Substrate (Bio-Rad) was used, and the images were scanned with the ChemiDoc XRS+ System and analyzed with Image Lab 6.0 (BioRad, both). The relative protein abundance in each sample was calculated using the "Relative quantity" tool implemented in Image Lab software, with glyceraldehyde-3-phosphate dehydrogenase (GAPDH) or alpha-Tubulin used as a reference.

Statistical analysis

P value was calculated by the Student t test for variables that followed normal distribution whereas for other the Mann-Whitney U test was applied. The calculations were made using Prism 9 (GraphPad, San Diego, CA, USA) software.

Results

Bortezomib-resistant MM cells show cross-resistance to carfilzomib

After continuous exposure to increasing concentrations of bortezomib or carfilzomib, we generated, from native MM1S WT cells, cell lines with acquired resistance to PIs - MM1S/R BTZ (cocultured with increasing concentrations of bortezomib) and MM1S/R CFZ (cocultured with increasing concentrations of carfilzomib). The resistance factor of MM1S/R BTZ cells equaled 2.93 - following 24-hour exposure to bortezomib IC_{50} equal to 15.2 nM for MM1S WT and 44.5 nM for MM1S/R BTZ. For the MM1S/R CFZ cell line, the resistance factor was 2.77; after exposure to carfilzomib, the IC_{50} was 8.3 nM for MM1S WT and 23.0 nM for MM1S/R CFZ. When exposed to different PIs than during the resistance generation period, MM1S/R BTZ cells were highly resistant to carfilzomib (IC_{50} = 43.5 nM), whereas MM1S/R CFZ (IC_{50} = 24.0 nM) cells were similarly sensitive to bortezomib as MM1S WT cells. The results are presented in **Figure 1**.

Proteomic profiling of bortezomib- and carfilzomib-resistant cells reveals different magnitudes of enrichment among similar pathways

Proteomic analysis identified 176 and 191 proteins significantly up-regulated, in comparison

to MM1S WT, in the MM1S/R BTZ and MM1S/R CFZ cell lines, respectively. In the same experiments 175 and 158 proteins were significantly down-regulated. Unsupervised PCA performed on the total number of proteins identified in three analyzed cell lines revealed that MM1S/R BTZ and MM1S/R CFZ differ significantly from MM1S WT cells and from each other, pointing toward different adaptations acquired in response to continuous bortezomib and carfilzomib exposure (**Figure 2C**). Canonical pathway analysis showed similar pathways enriched in both comparisons - MM1S WT vs. MM1S/R CFZ and MM1S WT vs. MM1S/R BTZ; however, important differences were present in terms of the statistical significance of particular pathways and the number of differentially expressed proteins (DEPs) associated with them (**Figure 2A**). The sirtuin signaling pathway was most enriched in bortezomib-resistant cells and among the top 4 pathways in carfilzomib-resistant cells. For the latter, the most significant difference was noted in EIF2 signaling, and interestingly, this pathway was the least significantly enriched in MM1S/R BTZ cells. Metabolic adaptations were observed in both MM1S/R BTZ and MM1S/R CFZ cells and included deregulation in glycolysis, gluconeogenesis, oxidative phosphorylation, tricarboxylic acid cycle and pathways associated with mitochondrial dysfunction - changes described previously as responsible for enhancing the ability of cells to counteract oxidoreductive stress [8, 9]. The unfolded protein response was enriched in both resistant MM1S cell lines. Both analyses showed important alterations in the protein ubiquitination pathway, which was further confirmed by comparing the accumulation of particular members of this pathway (**Figure 2B**), highlighting changes in the abundance of proteasome subunit-building proteins between all analyzed cell lines. Based on the abovementioned results and previous reports from the literature [21, 22], we focused on the functional analysis of proteasome function, redox homeostasis and UPR pathway activity.

Bortezomib and carfilzomib continue to block chymotrypsin-like activity of the proteasome in resistant cells

Following the proteomic results, we functionally validated changes in proteasome activity in all three experimental cell lines (MM1S WT, MM1S/R BTZ, MM1S/R CFZ). Carfilzomib and bortezomib preferentially block the β5 proteasome subunit responsible for chymotrypsin-like activity. The baseline activity of all three domains (chymotrypsin-, trypsin- and caspase-like) was significantly higher in the resistant cells. Our results also showed that in MM1S/R CFZ and MM1S/R BTZ, the drugs retained their ability to block the β5 subunit (**Figure 3**). Nevertheless, the relative reduction in chymotrypsin-like activity after incubation with 50 nM concentrations of the drugs was higher in sensitive than in resistant cells - 65% for MM1S/WT and bortezomib, 45% for MM1S/R BTZ, 96% for MM1S/WT and carfilzomib, 77% for MM1S/R CFZ. Carfilzomib and bortezomib do not block the function of the β2 and β1 subunits in either resistant or sensitive cells. The relative reduction of trypsin- and caspase-like activity was as follows: for bortezomib, respectively: -7% and 28% for MM1S WT, -1% and 24% for MM1S/R BTZ; for carfilzomib: 27% and 36% for MM1S WT, 20% and 18% in the case of MM1S WT/R CFZ.

Subsequently, we examined the dynamics of proteasome inhibition, apoptosis and cell viability after different durations of exposure to bortezomib and carfilzomib (**Figure 4**). Inhibition of chymotrypsin-like activity of proteasome starts early and remains stable during incubation. Caspase-3 activity was increased after 6 hours of incubation of the MM1S WT cell line with the highest concentration of drugs ($p = 0.0004$ for CFZ and $p = 0.007$ for BTZ). No significant changes in apoptotic activity in response to PIs were observed in MM1S/R BTZ or MM1s/CFZ cell lines. Significant changes in cell viability were detectable after 24 hours of incubation with drug concentrations ranging from 10 nM to 50 nM ($p < 0.01$, **Figures 1** and **4**).

Bortezomib- and carfilzomib-resistant cells differ in generation of reactive oxygen species

Several disruptions in pathways associated with the generation of reducing equivalents were described at the proteome level. To assess how these alterations affect the redox status of myeloma cells, we measured the generation of hydrogen peroxide induced by carfilzomib and bortezomib. Trend for lower signals in comparison to MM1S WT were seen in

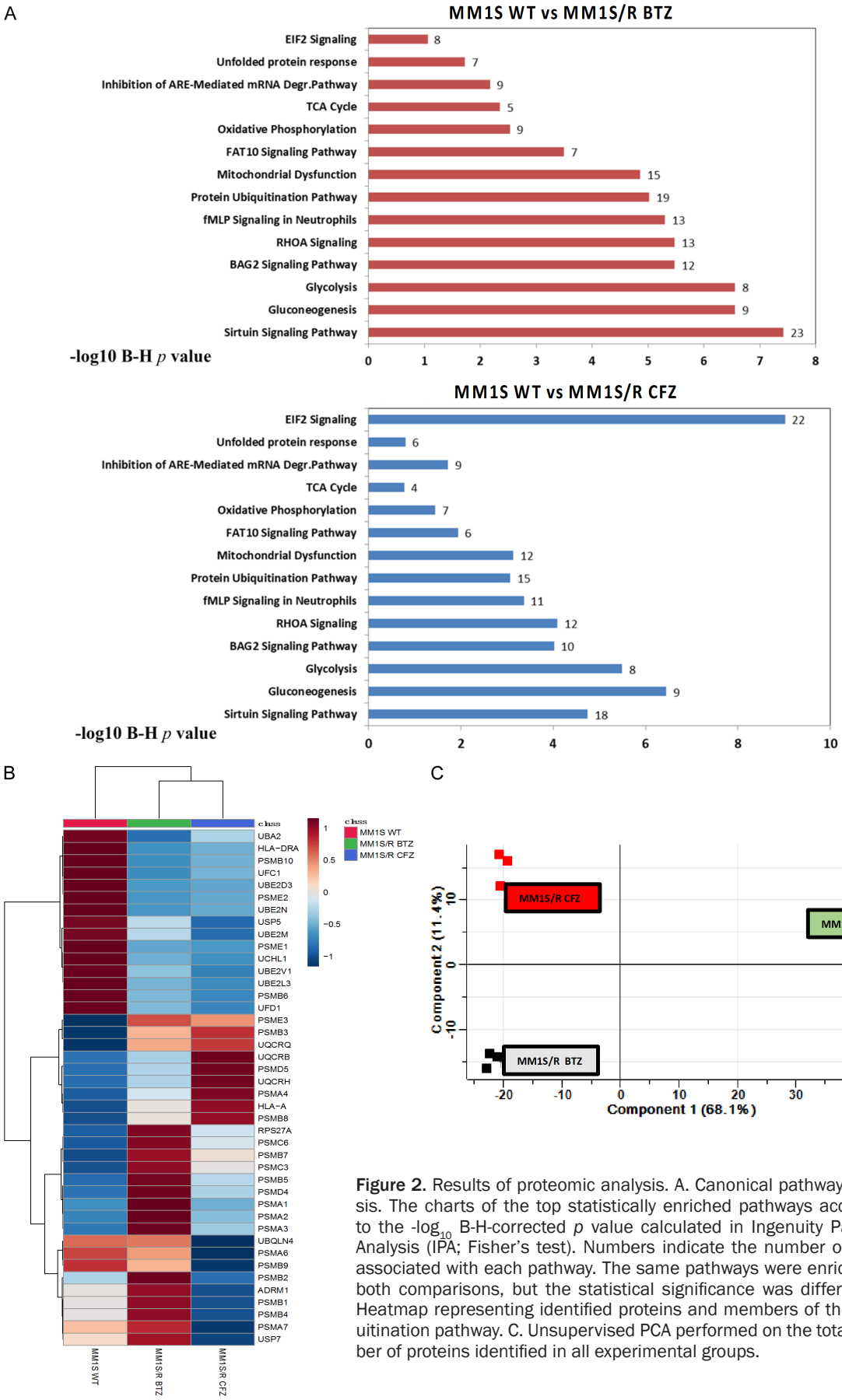

Figure 2. Results of proteomic analysis. A. Canonical pathway analysis. The charts of the top statistically enriched pathways according to the -$\log_{10}$ B-H-corrected p value calculated in Ingenuity Pathway Analysis (IPA; Fisher's test). Numbers indicate the number of DEPs associated with each pathway. The same pathways were enriched in both comparisons, but the statistical significance was different. B. Heatmap representing identified proteins and members of the ubiquitination pathway. C. Unsupervised PCA performed on the total number of proteins identified in all experimental groups.

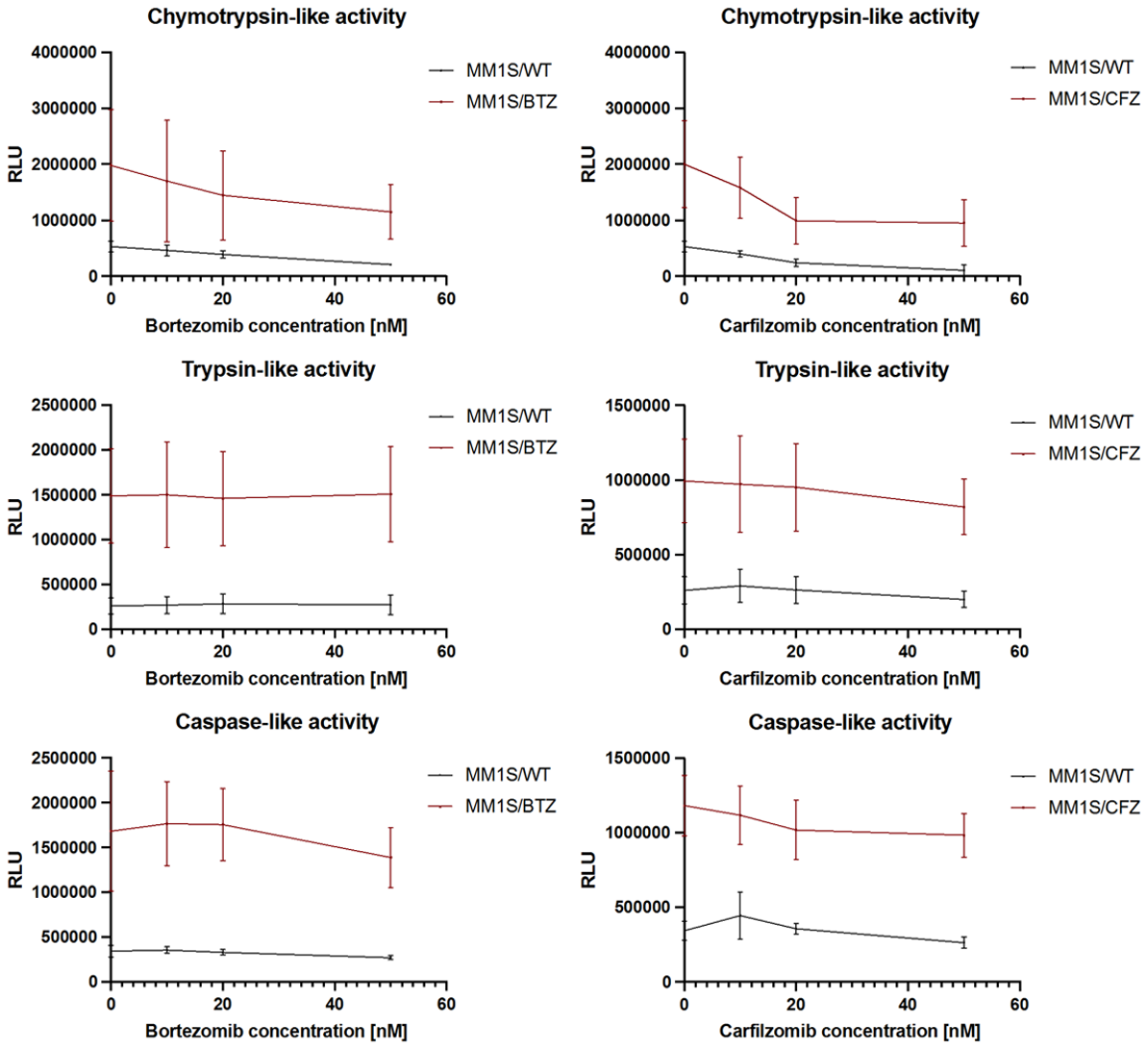

Figure 3. Proteasome activity after treatment with bortezomib and carfilzomib. Chymotrypsin-, trypsin- and caspase-like protease activities were measured after 6 hours of incubation with the drugs.

MM1S/R BTZ cells ($p > 0.05$), whereas MM1S/R CFZ cells in drug-free medium generate more ROS than sensitive cells ($p < 0.0001$). Drug-induced ROS generation increased only in MM1S WT cells after incubation with high concentrations of carfilzomib ($p = 0.015$ for 50 nM carfilzomib vs. medium), in PI-resistant cell lines and after incubation with bortezomib, drug concentration did not affect the results (**Figure 5**).

PI-resistant cells show similar upregulation in unfolded protein response pathway activity

To further investigate adjustments in the activity of the unfolded protein response pathway, the relative abundance of key proteins associated with this network was measured. The measurements included baseline status in a drug-free medium as well as changes arising over time after incubation with carfilzomib or bortezomib at different concentrations (**Figure 6**). In general, a higher level of accumulation of all analyzed proteins was observed in resistant lines compared to their sensitive counterparts. At baseline, MM1S/R BTZ and MM1S/R CFZ cells showed similar alterations when compared to MM1S WT cells. The accumulation of XBP1s and IRE1 was higher in PI-resistant cells than in their sensitive counterparts. For the ATF6 effector arm, the protein accumulation was higher in carfilzomib-resistant cell lines. Downstream effectors of PERK showed discrepant results. ATF4 was overrepresented in both resistant cell lines, while eIF2α protein

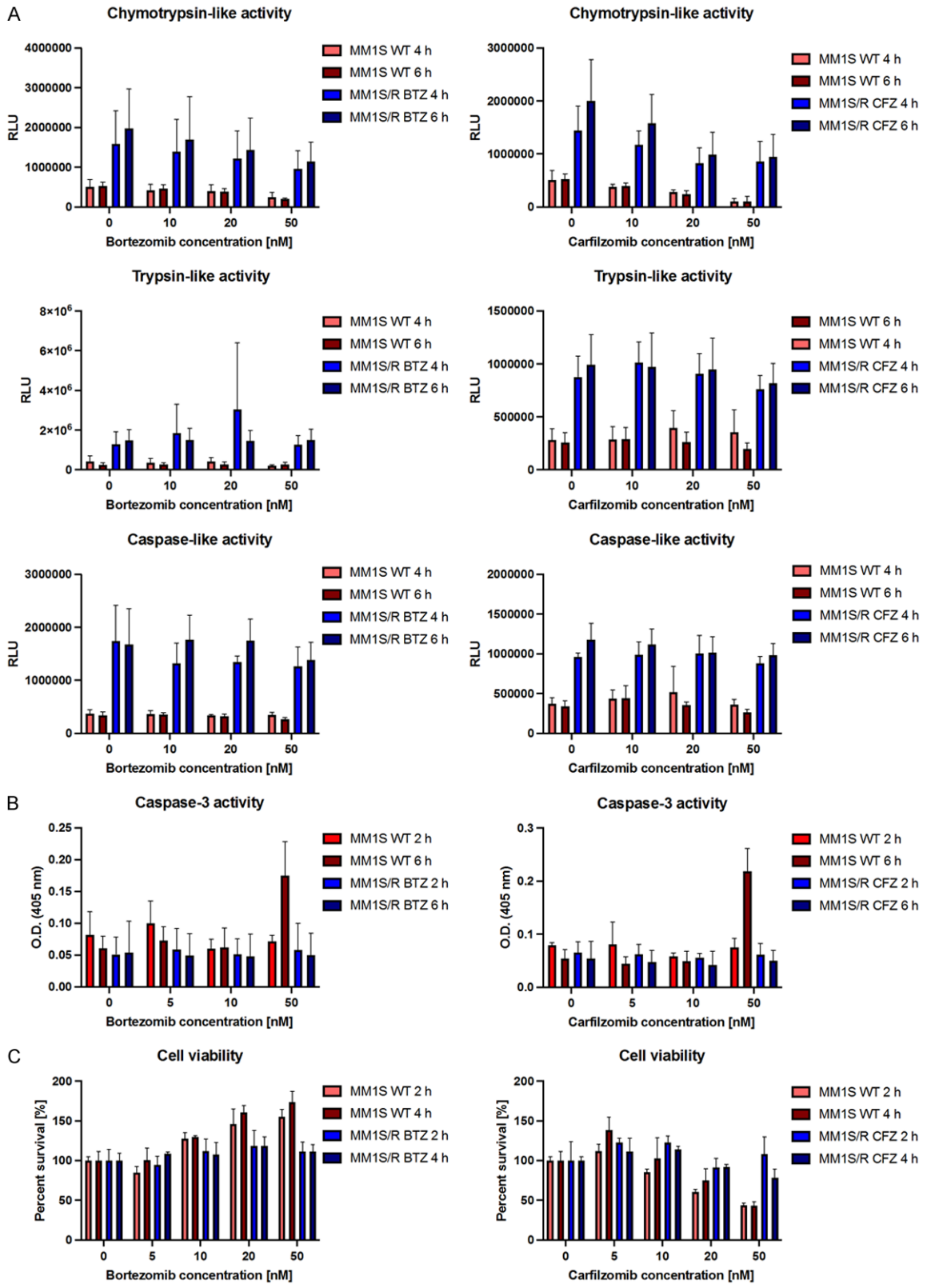

Figure 4. Changes in proteasome activity and cell viability over time. A. Chymotrypsin-like protease activity is blocked after 4 hours of incubation with drug and remains stable after 6 hours. Trypsin- and caspase-like activities remained intact at both timepoints. B. Proteasome inhibition by 50 nM bortezomib and carfilzomib triggers apoptosis in sensitive cells after 6 hours of incubation. C. Cell viability was not affected after 4 hours of incubation.

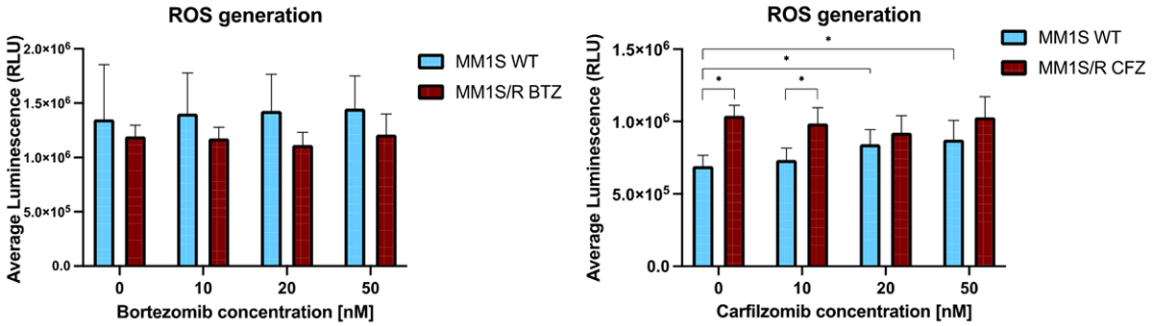

Figure 5. Reactive oxygen species generation. Bortezomib-resistant cells exhibit lower concentrations of hydrogen peroxide in comparison to sensitive cells. The amount of hydrogen peroxide after 6 hours of incubation was not affected by the drug concentration. Statistically significant differences are marked with (*).

abundance, in comparison to MM1S WT, was consistently higher only in MM1S/R CFZ.

Measuring the abundance of UPR proteins at different time points and different drug concentrations enabled dynamic characterization of adaptations in the UPR present in resistant cell lines. In both resistant cell lines, higher activity of the three effector arms of the UPR was observed; however, there were some differences between carfilzomib- and bortezomib-resistant cells. In MM1S/R BTZ, IRE1 abundance decreased with time of exposure and with increasing drug concentrations. This change was followed by an increase in the abundance of downstream effectors of this arm - pIRE1 and XBP1s. In MM1S/WT CFZ, we did not observe such changes for IRE1 or similarly for pIRE1. However, an increase in abundance was seen for XBP1s. Enhancement of the activity of the second arm, initiated by PERK phosphorylation, in resistant cell lines was detected to a lesser extent. A tendency was seen in the increase in the abundance of the downstream effector protein ATF4 at both analyzed time points for bortezomib-resistant cells and after 2 hours of incubation in carfilzomib-resistant cells. There were no clear tendencies in the abundances of two other analyzed proteins in this pathway - eIF2α and NRF2. Finally, ATF6 consistently increased with drug concentration in the MM1S/R BTZ cell line to a higher extent than in sensitive cells. These changes were also observed in MM1S/R CFZ cells.

Altogether, these results show that PI-resistant cells generated in this project exhibit higher UPR activity than sensitive cells, present both at baseline and in response to carfilzomib or bortezomib treatment and includes all three axes of UPR signaling.

Discussion

Several studies in recent years have aimed to describe the mechanisms responsible for resistance to bortezomib and carfilzomib, leading to different, sometimes contradictory, conclusions. This confusion can be attributed to biological discrepancies between experimental cell lines that, as was recently proven, differ significantly in reflecting processes occurring *in vivo* in myeloma cells from patients [23]. The MM1S cell line that we used in this project is among those that most closely resemble actual patient tumors. PI-resistant cells generated from MM1S were not extensively studied in the past, with the exception of ixazomib-resistant cells [24].

Our results show that while sharing several similarities, bortezomib- and carfilzomib-resistant myeloma cells acquire different adaptations. These discrepancies result in the unidirectional cross-resistance observed in our experiments. Intriguingly, this unidirectional cross-resistance applies only to MM1S/R BTZ being resistant to carfilzomib, which can be attributed to more mechanistic causes of carfilzomib resistance observed *in vitro*, linked to p-glycoprotein overexpression [25]. Our results also showed lower ROS generation in bortezomib-resistant cells. We do not provide any direct explanation for this phenomenon in our study, but this can be linked to the higher enrichment of glycolysis and the tricarboxylic acid cycle in MM1S/R BTZ cells than in MM1S/R

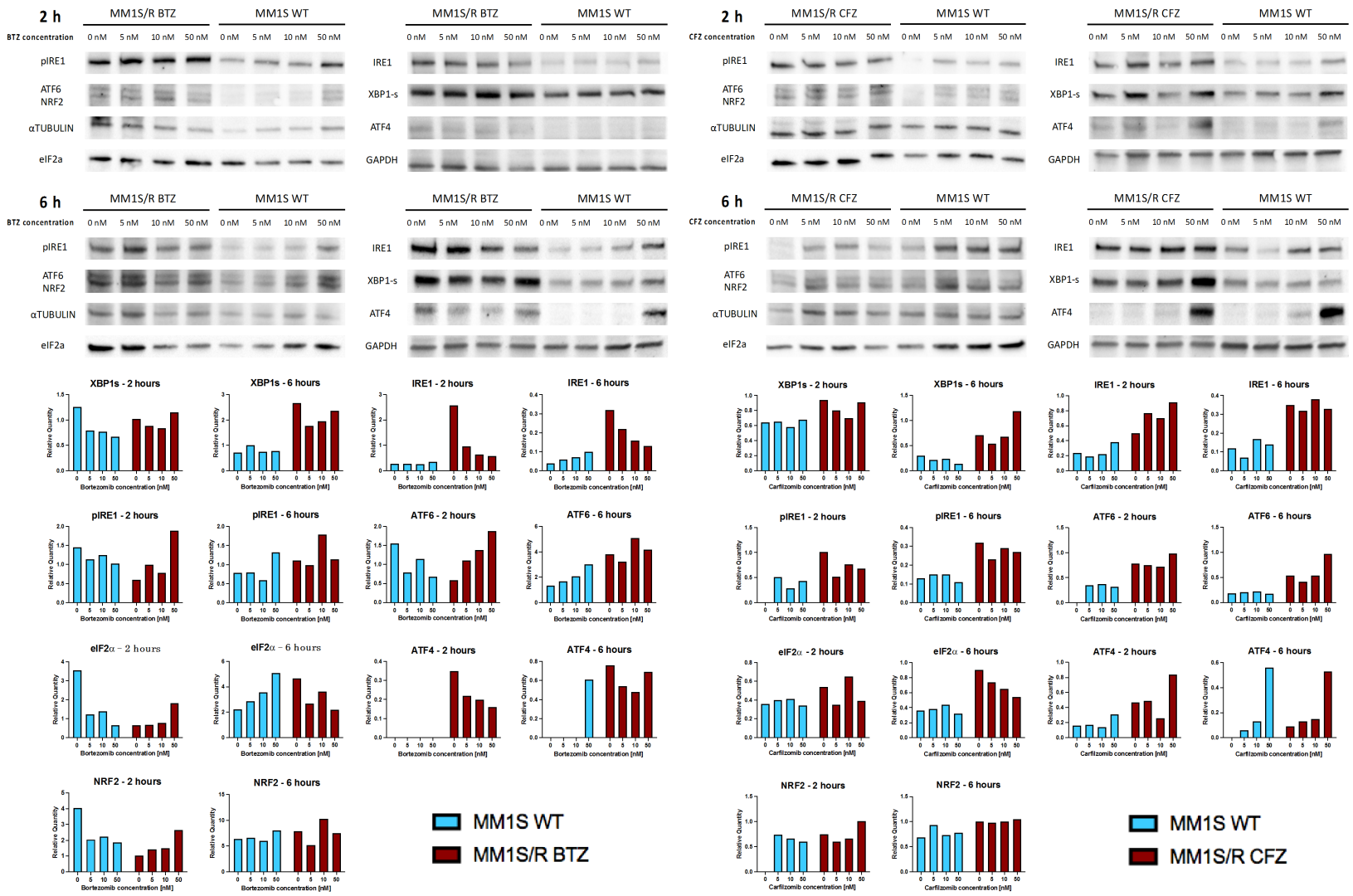

Figure 6. UPR pathway activity. Western blots present the abundance of key proteins involved in UPR signaling and its change as a function of drug concentration (bortezomib - left panel, carfilzomib - right panel) and time of incubation (2 and 6 hours). Bar graphs show the relative quantity of the analyzed proteins.

CFZ cells. The activity of these pathways provides reducing equivalents (e.g., nicotinamide adenine dinucleotide phosphate (NADPH)), leading to the increased capability of MM1S/R BTZ cells to maintain redox homeostasis and allowing for resistance to both drugs. In clinical practice, carfilzomib is usually utilized after bortezomib-based therapies, and the activity of bortezomib in patients exposed previously to carfilzomib has not been investigated. Being aware of all the limitations of our study, we speculate that such a reverse strategy appears to be interesting to explore in the future.

Similar to previous reports, our results suggest that both bortezomib and carfilzomib retain the ability to block the chymotrypsin-like activity of the proteasome [26]. However, the baseline activity of all three catalytic sites of the proteasome is significantly higher in PI-resistant cells, so even in the presence of β5 subunit inhibition, the chymotrypsin-like activity remains much higher than in the sensitive cells. Intriguingly, proteomic results suggest that this effect may be mediated by different adaptations in the ubiquitin-proteasome pathway in bortezomib-resistant cells than in carfilzomib-resistant cells. Nevertheless, the net effect of higher proteasomal activity remains the same for both cell lines. We identified a similar upregulation of proteasome activity in a previous study conducted on MM patient-derived plasma cells [12].

In proteomic profiling, the sirtuin signaling pathway was identified as the most dysregulated in bortezomib-resistant cells and important in carfilzomib-resistant cells. Sirtuins are enzymes with histone deacetylase activity coordinating the expression of genes responsible for a plethora of cellular processes, including DNA repair, response to stress and cell metabolism [27]. Interestingly, sirtuins can also be responsible for attenuation of UPR activity [28]. The interplay of sirtuin signaling with UPR effectors to enhance its ability to respond to ER stress while decreasing proapoptotic pathway activity requires further study.

For carfilzomib-resistant cells, the most significant differences involved eIF2 signaling. Proteins from this group are responsible for the initiation of translation by delivering tRNA to ribosomes. Their important role in the context of myeloma cells is in responding to unfolded protein response activation by global attenuation of translation [14]. These results are in line with the identified dysregulations in the UPR pathway in carfilzomib-resistant cells. However, contrary to some other reports, we did not observe decreased UPR activity. Particularly interesting was the enhanced activity of the ATF6 arm of this pathway, which was previously not considered important [29]. Here, we show that the relative accumulation of this protein increases proportionally with drug concentrations and is higher than the relative accumulation of this protein in sensitive cells in both MM1S/R BTZ and MM1S/R CFZ cells. ATF6 modulates the UPR by enhancing XBP1 gene transcription, and by direct heterodimerization with the XBP1 protein, ATF6 induces the activity of pathways responsible for ER-associated degradation of proteins [30]. The UPR is well known to be a “double-edged sword” whose activation can ultimately lead to cell death. ATF6, however, is not directly involved in initiating apoptotic reactions [31]. Based on our results, we speculate that IRE1/XPB1-low is only one of the possible phenotypes of PI-resistant myeloma cells. During clonal evolution, cells can acquire other adaptations. The IRE1/XBP1-low signature is connected with decreased monoclonal protein production [16]; however, this oligosecretory pattern is not exclusive in patients with refractory/relapsed MM. The MM1S/R cells generated in this project appear to show an increased ability to respond with UPR activation to PI-induced proteotoxicity which, in concert with higher proteasomal capacity, changes in the protein ubiquitination pathway and metabolic adaptations give the cells a survival advantage over their sensitive counterparts even though relative proteasome inhibition is similar in all three cell lines.

This study has some limitations that should be underlined. It was conducted on one myeloma cell line and was not validated on plasma cells derived from MM patients. Such tests are necessary to assess if these results have potential clinical significance. Also, only some dysregulated pathways identified in the proteomic analysis were further analyzed in the functional studies, especially role of sirtuin signaling and metabolic adaptations require additional investigation in the context of resistance to proteasome inhibitors in MM.

In conclusion, the results of this study warrant further research on the role of UPR signaling in resistance to PIs. Clinical validation of these findings is highly anticipated, potentially leading to distinguishing patients with low and high UPR activity. Such characterization may be important for future tailoring of individualized approaches to augment bortezomib and carfilzomib efficacy.

Acknowledgements

This study was supported by the Polish National Science Center grants: 2018/29/N/NZ5/00651 to Tadeusz Kubicki and 2017/25/B/NZ5/01827 to Dominik Dytfeld.

Disclosure of conflict of interest

None.

Address correspondence to: Dominik Dytfeld, Department of Hematology and Bone Marrow Transplantation, Poznan University of Medical Sciences, Poznan, Poland. E-mail: dytfeld@me.com

References

[1] Ravi P, Kumar SK, Cerhan JR, Maurer MJ, Dingli D, Ansell SM and Rajkumar SV. Defining cure in multiple myeloma: a comparative study of outcomes of young individuals with myeloma and curable hematologic malignancies. Blood Cancer J 2018; 28: 26.

[2] Yong K, Delforge M, Driessen C, Fink L, Flinois A, Gonzalez-McQuire S, Safaei R, Karlin L, Mateos MV, Raab MS, Schoen P and Cavo M. Multiple myeloma: patient outcomes in real-world practice. Br J Haematol 2016; 175: 252-264.

[3] Stewart AK, Rajkumar SV, Dimopoulos MA, Masszi T, Špička I, Oriol A, Hájek R, Rosiñol L, Siegel DS, Mihaylov GG, Goranova-Marinova V, Rajnics P, Suvorov A, Niesvizky R, Jakubowiak AJ, San-Miguel JF, Ludwig H, Wang M, Maisnar V, Minarik J, Bensinger WI, Mateos MV, Ben-Yehuda D, Kukreti V, Zojwalla N, Tonda ME, Yang X, Xing B, Moreau P and Palumbo A; ASPIRE Investigators. Carfilzomib, lenalidomide, and dexamethasone for relapsed multiple myeloma. N Engl J Med 2015; 372: 142-152.

[4] Moreau P, Masszi T, Grzasko N, Bahlis NJ, Hansson M, Pour L, Sandhu I, Ganly P, Baker BW, Jackson SR, Stoppa AM, Simpson DR, Gimsing P, Palumbo A, Garderet L, Cavo M, Kumar S, Touzeau C, Buadi FK, Laubach JP, Berg DT, Lin J, Di Bacco A, Hui AM, van de Velde H and Richardson PG. Oral ixazomib, lenalidomide, and dexamethasone for multiple myeloma. N Engl J Med 2016; 374: 1621-1634.

[5] Richardson PG, Sonneveld P, Schuster MW, Irwin D, Stadtmauer EA, Facon T, Harousseau JL, Ben-Yehuda D, Lonial S, Goldschmidt H, Reece D, San-Miguel JF, Bladé J, Boccadoro M, Cavenagh J, Dalton WS, Boral AL, Esseltine DL, Porter JB, Schenkein D and Anderson KC; Assessment of Proteasome Inhibition for Extending Remissions (APEX) Investigators. Bortezomib or high-dose dexamethasone for relapsed multiple myeloma. N Engl J Med 2005; 352: 2487-2498.

[6] Ito S. Proteasome inhibitors for the treatment of multiple myeloma. Cancers 2020; 12: 265.

[7] Ri M, Iida S, Nakashima T, Miyazaki H, Mori F, Ito A, Inagaki A, Kusumoto S, Ishida T, Komatsu H, Shiotsu Y and Ueda R. Bortezomib-resistant myeloma cell lines: a role for mutated PSMB5 in preventing the accumulation of unfolded proteins and fatal ER stress. Leukemia 2010; 24: 1506-12.

[8] Besse L, Besse A, Mendez-Lopez M, Vasickova K, Sedlackova M, Vanhara P, Kraus M, Bader J, Ferreira RB, Castellano RK, Law BK and Driessen C. A metabolic switch in proteasome inhibitor-resistant multiple myeloma ensures higher mitochondrial metabolism, protein folding and sphingomyelin synthesis. Haematologica 2019; 104: e415-419.

[9] Soriano GP, Besse L, Li N, Kraus M, Besse A, Meeuwenoord N, Bader J, Everts B, den Dulk H, Overkleeft HS, Florea BI and Driessen C. Proteasome inhibitor-adapted myeloma cells are largely independent from proteasome activity and show complex proteomic changes, in particular in redox and energy metabolism. Leukemia 2016; 30: 2198-2207.

[10] Barrio S, Stühmer T, Da-Viá M, Barrio-Garcia C, Lehners N, Besse A, Cuenca I, Garitano-Trojaola A, Fink S, Leich E, Chatterjee M, Driessen C, Martinez-Lopez J, Rosenwald A, Beckmann R, Bargou RC, Braggio E, Stewart AK, Raab MS, Einsele H and Kortüm KM. Spectrum and functional validation of PSMB5 mutations in multiple myeloma. Leukemia 2019; 33: 447-456.

[11] Caillot M, Dakik H, Mazurier F and Sola B. Targeting reactive oxygen species metabolism to induce myeloma cell death. Cancers 2021; 13: 2411.

[12] Dytfeld D, Luczak M, Wrobel T, Usnarska-Zubkiewicz L, Brzezniakiewicz K, Jamroziak K, Giannopoulos K, Przybylowicz-Chalecka A, Ratajczak B, Czerwinska-Rybak J, Nowicki A, Joks M, Czechowska E, Zawartko M, Szczepaniak T, Grzasko N, Morawska M, Bochenek M, Kubicki T, Morawska M, Tusznio K, Jakubowiak A and Komarnicki MA. Comparative proteomic profiling of refractory/relapsed multiple myeloma

reveals biomarkers involved in resistance to bortezomib-based therapy. Oncotarget 2016; 7: 56726-56736.
[13] Cenci S and Sitia R. Managing and exploiting stress in the antibody factory. FEBS Lett 2007; 581: 3652-7.
[14] Hetz C and Papa FR. The unfolded protein response and cell fate control. Mol Cell 2018; 69: 169-181.
[15] Obeng EA, Carlson LM, Gutman DM, Harrington WJ, Lee KP and Boise LH. Proteasome inhibitors induce a terminal unfolded protein response in multiple myeloma cells. Blood 2006; 107: 4907-4916.
[16] Leung-Hagesteijn C, Erdmann N, Cheung G, Keats JJ, Stewart AK, Reece DE, Chung KC and Tiedemann RE. Xbp1s-negative tumor B cells and pre-plasmablasts mediate therapeutic proteasome inhibitor resistance in multiple myeloma. Cancer Cell 2013; 24: 289-304.
[17] Gambella M, Rocci A, Passera R, Gay F, Omedè P, Crippa C, Corradini P, Romano A, Rossi D, Ladetto M, Boccadoro M and Palumbo A. High XBP1 expression is a marker of better outcome in multiple myeloma patients treated with bortezomib. Haematologica 2014; 99: e14-16.
[18] Borjan B, Kern J, Steiner N, Gunsilius E, Wolf D and Untergasser G. Spliced XBP1 levels determine sensitivity of multiple myeloma cells to proteasome inhibitor bortezomib independent of the unfolded protein response mediator GRP78. Front Oncol 2020; 9: 1530.
[19] Luczak M, Suszynska-Zajczyk J, Marczak L, Formanowicz D, Pawliczak E, Wanic-Kossowska M and Stobiecki M. Label-Free quantitative proteomics reveals differences in molecular mechanism of atherosclerosis related and non-related to chronic kidney disease. Int J Mol Sci 2016; 17: 631.
[20] Bradford MM. A rapid and sensitive method for the quantitation of microgram quantities of protein utilizing the principle of protein-dye binding. Anal Biochem 1976; 72: 248-254.
[21] Kubicki T, Gil L and Dytfeld D. Endoplasmic reticulum stress and proteasome inhibitors in multiple myeloma: room for improvement. Pol Arch Intern Med 2021; 131: 361-368.
[22] Wallington-Beddoe CT, Sobieraj-Teague M, Kuss BJ and Pitson SM. Resistance to proteasome inhibitors and other targeted therapies in myeloma. Br J Haematol 2018; 182: 11-28.
[23] Sarin V, Yu K, Ferguson ID, Gugliemini O, Nix MA, Hann B, Sirota M and Wiita AP. Evaluating the efficacy of multiple myeloma cell lines as models for patient tumors via transcriptomic correlation analysis. Leukemia 2020; 34: 2754-2765.
[24] Brünnert D, Kraus M, Stühmer T, Kirner S, Heiden R, Goyal P, Driessen C, Bargou RC and Chatterjee M. Novel cell line models to study mechanisms and overcoming strategies of proteasome inhibitor resistance in multiple myeloma. Biochim Biophys Acta Mol Basis Dis 2019; 1865: 1666-1676.
[25] Ao L, Wu Y, Kim D, Jang ER, Kim K, Lee DM, Kim KB and Lee W. Development of peptide-based reversing agents for p-glycoprotein-mediated resistance to carfilzomib. Mol Pharm 2012; 9: 2197-205.
[26] Zaal EA, Wu W, Jansen G, Zweegman S, Cloos J and Berkers CR. Bortezomib resistance in multiple myeloma is associated with increased serine synthesis. Cancer Metab 2017; 5: 7.
[27] Haigis MC and Sinclair DA. Mammalian Sirtuins: biological insights and disease relevance. Annu Rev Pathol 2010; 5: 253-95.
[28] Sadia K, Ashraf MZ and Mishra A. Therapeutic role of sirtuins targeting unfolded protein response, coagulation, and inflammation in hypoxia-induced thrombosis. Front Physiol 2021; 12: 733453.
[29] Xiong S, Chng WJ and Zhou J. Crosstalk between endoplasmic reticulum stress and oxidative stress: a dynamic duo in multiple myeloma. Cell Mol Life Sci 2021; 78: 3883-3906.
[30] Yamamoto K, Sato T, Matsui T, Sato M, Okada T, Yoshida H, Harada A and Mori K. Transcriptional induction of mammalian ER quality control proteins is mediated by single or combined action of ATF6α and XBP1. Dev Cell 2007; 13: 365-76.
[31] Urra H, Dufey E, Lisbona F, Rojas-Rivera D and Hetz C. When ER stress reaches a dead end. Biochim Biophys Acta 2013; 1833: 3507-3517.